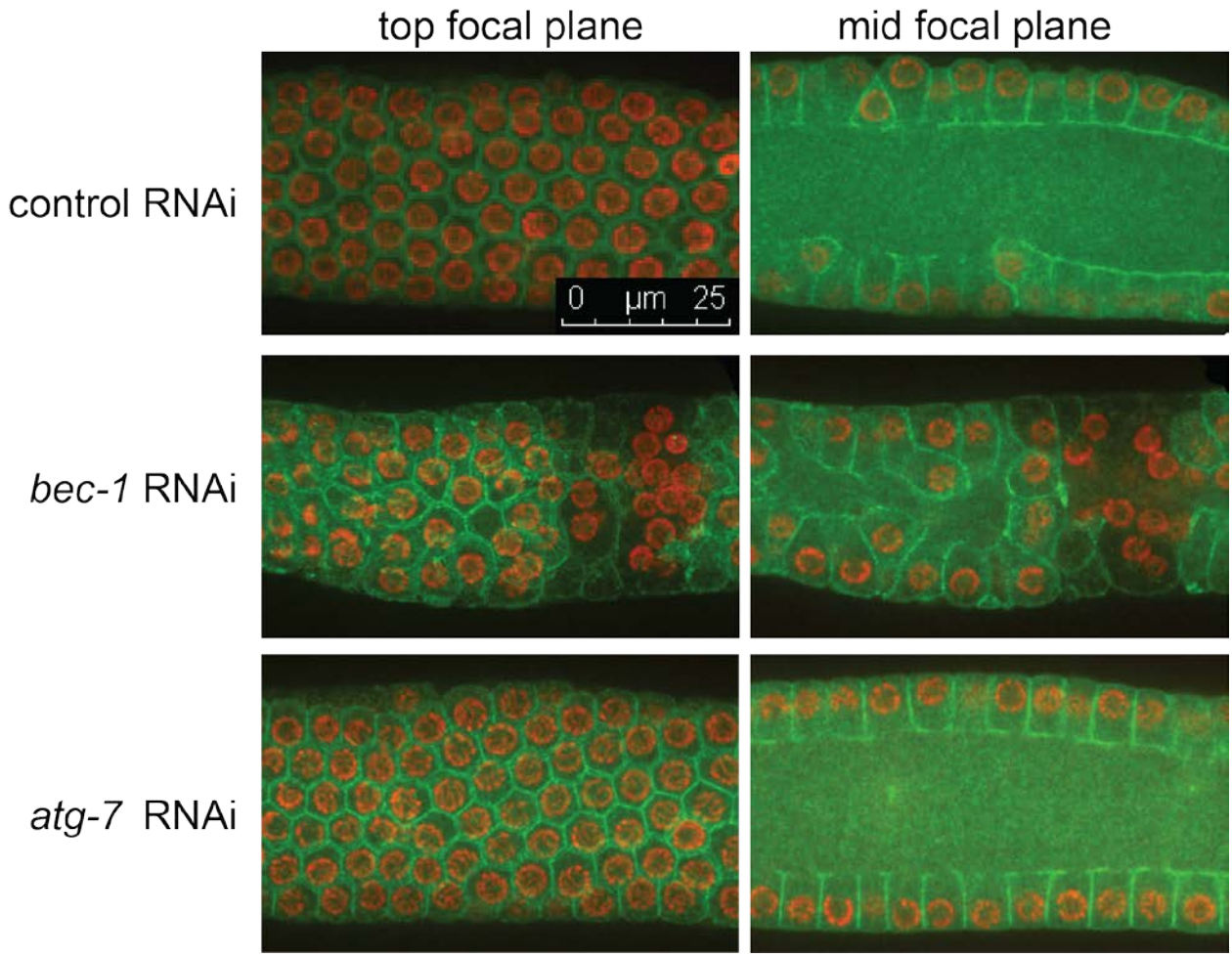

Figure S1. BEC-1 and ATG-7 are necessary for membrane organization. ***Related to Figure 1.***
Representative gonad confocal images of animals that express the plasma membrane GFP::PH$^{PLC1\delta1}$ reporter, to visualize the plasma membrane, treated with *bec-1* or *atg-7 RNAi.* Plasmid (L4440) served as a negative control. The germline membrane of control animals forms hexagonal shapes of equal size (top focal plane), and a T-shape morphology (mid focal plane). In *bec-1* RNAi treated animals, the germline defects on the membrane are visible in the top and mid focal planes (also see Figure S4E). The *bec-1* RNAi treated animals have lost the T-shapes (midfocal plane), and multiple multinucleated cells collapsed into the rachis. *atg-7* RNAi treated animals have the hexagonal shapes of equal size, however the cells do not appear to be dividing, or the polarity is affected because no cells have changed shape.

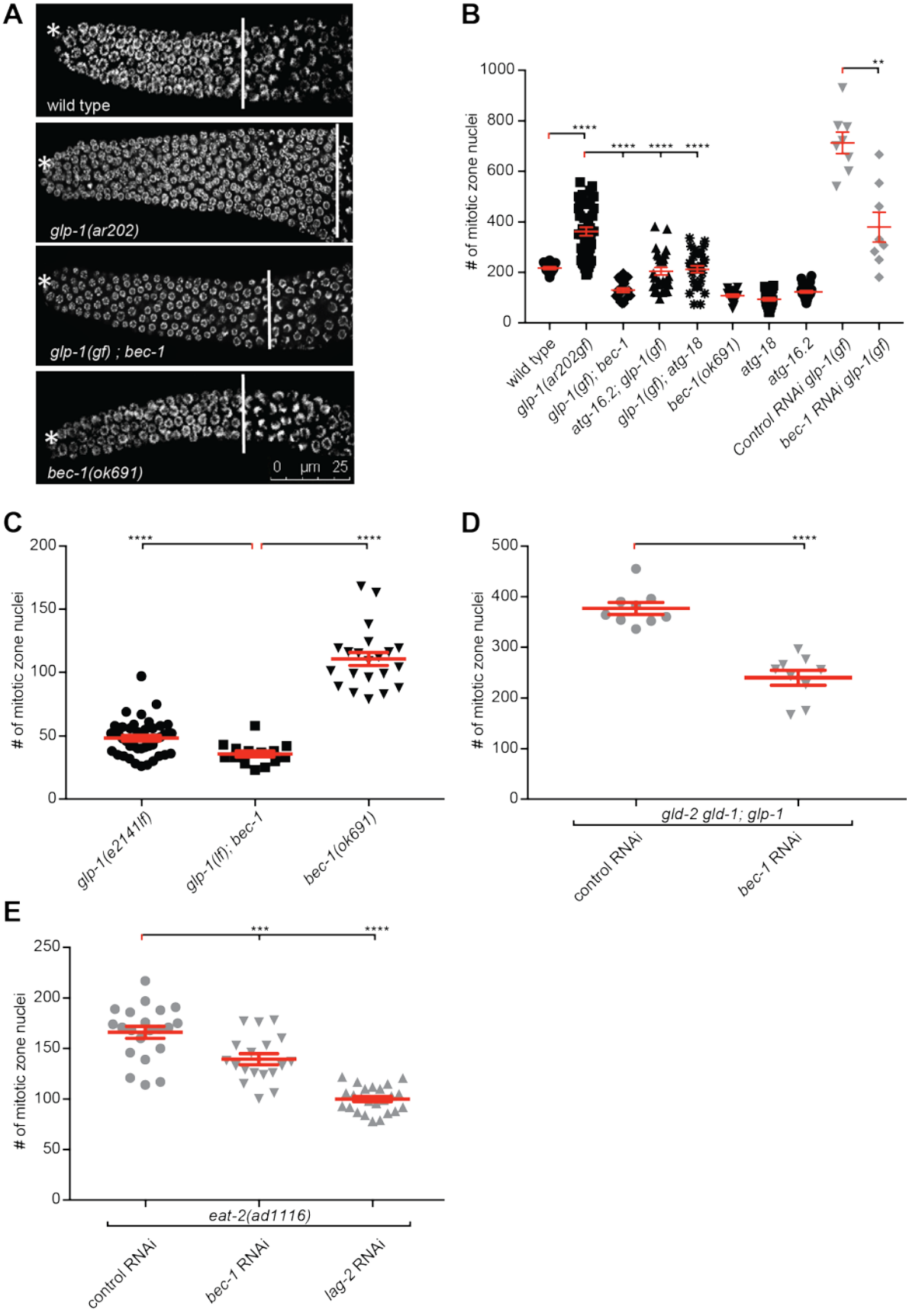
A
wild type
glp-1(ar202)
glp-1(gf) ; bec-1
bec-1(ok691)
0 µm 25
B
# of mitotic zone nuclei
1000
800
600
400
200
0
****
****
****
****
**
wild type
glp-1(ar202gf)
glp-1(gf); bec-1
atg-16.2; glp-1(gf)
glp-1(gf); atg-18
bec-1(ok691)
atg-18
atg-16.2
Control RNAi glp-1(gf)
bec-1 RNAi glp-1(gf)
C
# of mitotic zone nuclei
200
150
100
50
0
****
****
glp-1(e2141lf)
glp-1(lf); bec-1
bec-1(ok691)
D
# of mitotic zone nuclei
500
400
300
200
100
0
****
gld-2 gld-1; glp-1
control RNAi
bec-1 RNAi
E
# of mitotic zone nuclei
250
200
150
100
50
0
***
****
eat-2(ad1116)
control RNAi
bec-1 RNAi
lag-2 RNAi

Figure S2. BEC-1 acts independently of the GLP-1/Notch, TGFβ/DAF-7 signaling and dietary restriction pathway. *Related to Figure 2.*

(A) Representative confocal images of DAPI stained gonads of wild type, *glp-1(ar202gf), bec-1(ok691),* and *glp-1(ar202gf);bec-1(ok691)* double mutants. * labels the distal tip of the gonad. White line marks the end of the mitotic zone. **(B)** Quantification of mitotic zone nuclei in the proliferative zone of wild type, *glp-1(ar202gf)* single mutant animals, *glp-1(ar202gf);bec-1(ok691), glp-1(ar202gf);atg-18(gk378), atg-16.2(ok3224); glp-1(ar202gf)* double mutants and in *bec-1(ok691), atg-18(gk378),* or *atg-16.2(ok3224)* single mutants, as well as in the *glp-1(ar202)* mutant animals RNAi depleted of *bec-1* activity or control (gray symbols). **(C)** Quantification of mitotic zone nuclei in the proliferative zone of *glp-1(e2141lf), glp-1(e2141lf);bec-1(ok691)* and *bec-1(ok691)* animals. **(D)** Number of mitotic zone nuclei in animals segregating from *gld-2(q497) gld-1(q485)/hT2 [dpy-18(h662)] I; unc-32(e189) glp-1(q175)/hT2 [bli-4(e937)] III* after RNAi depletion of *bec-1* or with control plasmid (L4440). **(E)** Number of mitotic zone nuclei in the *eat-2(ad1116)* dietary restricted animals treated with *bec-1* or *lag-2* RNAi (as a positive control), as well as with control plasmid (L4440; as a negative control). For (A-E), animals were raised at 15ºC and switched to 25ºC as L3 larvae. Young adults were DAPI stained and analyzed. Results reflect the average of at least three biological replicates shown as the mean ± SEM (shown as error bars). Number of analyzed gonads N≥30. Statistical significance was determined by one-way ANOVA with corrections for multiple comparisons using the method of Tukey (B, C) or Šídák (E). Statistical significance of individual comparisons in (D) was determined with the Mann-Whitney test; *** P≤0.001, **** P≤0.0001, ns- not significant.

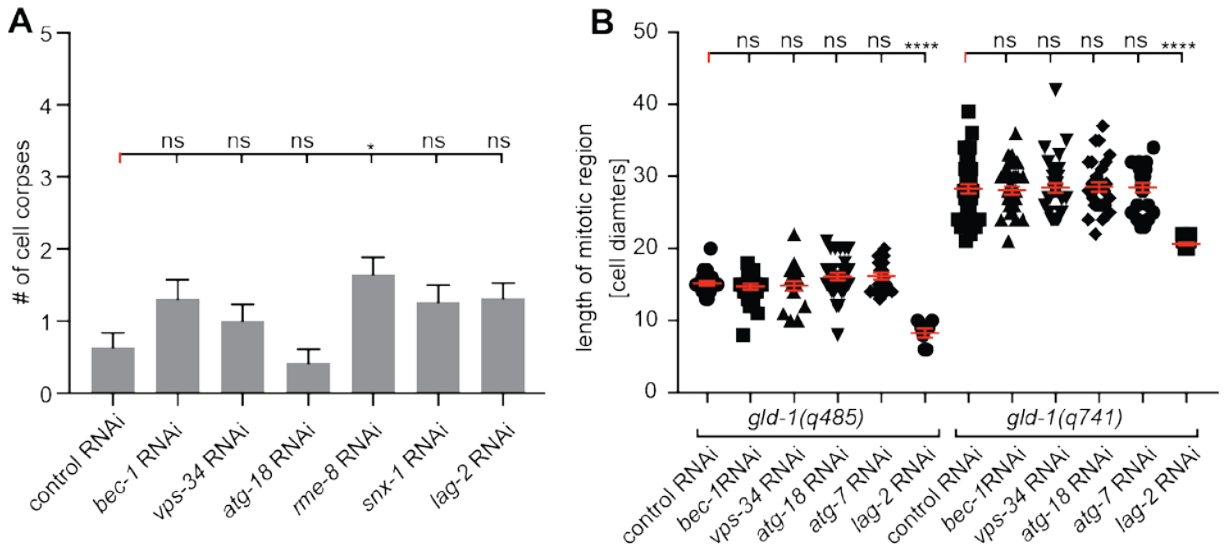

Figure S3. Autophagy genes are not required for germ cell survival or the cell decision to switch from proliferation to differentiation. *Related to Figure 3.*

(A) Quantification of the apoptotic cell corpses at the gonad bend. Animals that carry a *ced-1::gfp* transgene ***(****bcIs39)* labeling apoptotic nuclei were treated with RNAi against the control *(L4440), bec-1, vps-34, atg-18, rme-8, snx-1* or *lag-2* activity. Animals raised at 20°C and analyzed as young adults. **(B)** Quantification of the mitotic region length measured in cell diameters of *gld-1(q485)* or *gld-3(q741)* mutants after RNAi depletion with control (L4440), *bec-1, vps-34, atg-18, atg-7* or *lag-2* (as a positive control). For (B), animals were grown at 15°C switched to 20°C at L1 larval stage and analyzed as young adults**.** For (A), and (B), results reflect the average of at least three replicates shown as the mean ± SEM (shown as error bars). Number of analyzed gonads N>20. Statistical significance was determined by one-way ANOVA with corrections for multiple comparisons using the method of Tukey, and indicated as * P ≤0.05, **** P≤0.0001, ns - not significant.

NOTE: Strain used in (A) MD701: *bcIs39[lim-7p::ced-1p::GFP+lin-15(+)]* that expresses functional CED-1::GFP protein in the sheath cells. In (B), *gld-1(q485)* animals were segregated from the strain JK3025: *gld1(q485)I/hT2[bli-4(e937) let?(q782)qIs48](I;III),* and *gld-3(q741)* animals were segregated from the strain JK 3345: *gld-3(q741)/mIn1[mIs14 dpy-10(e128)] II.*

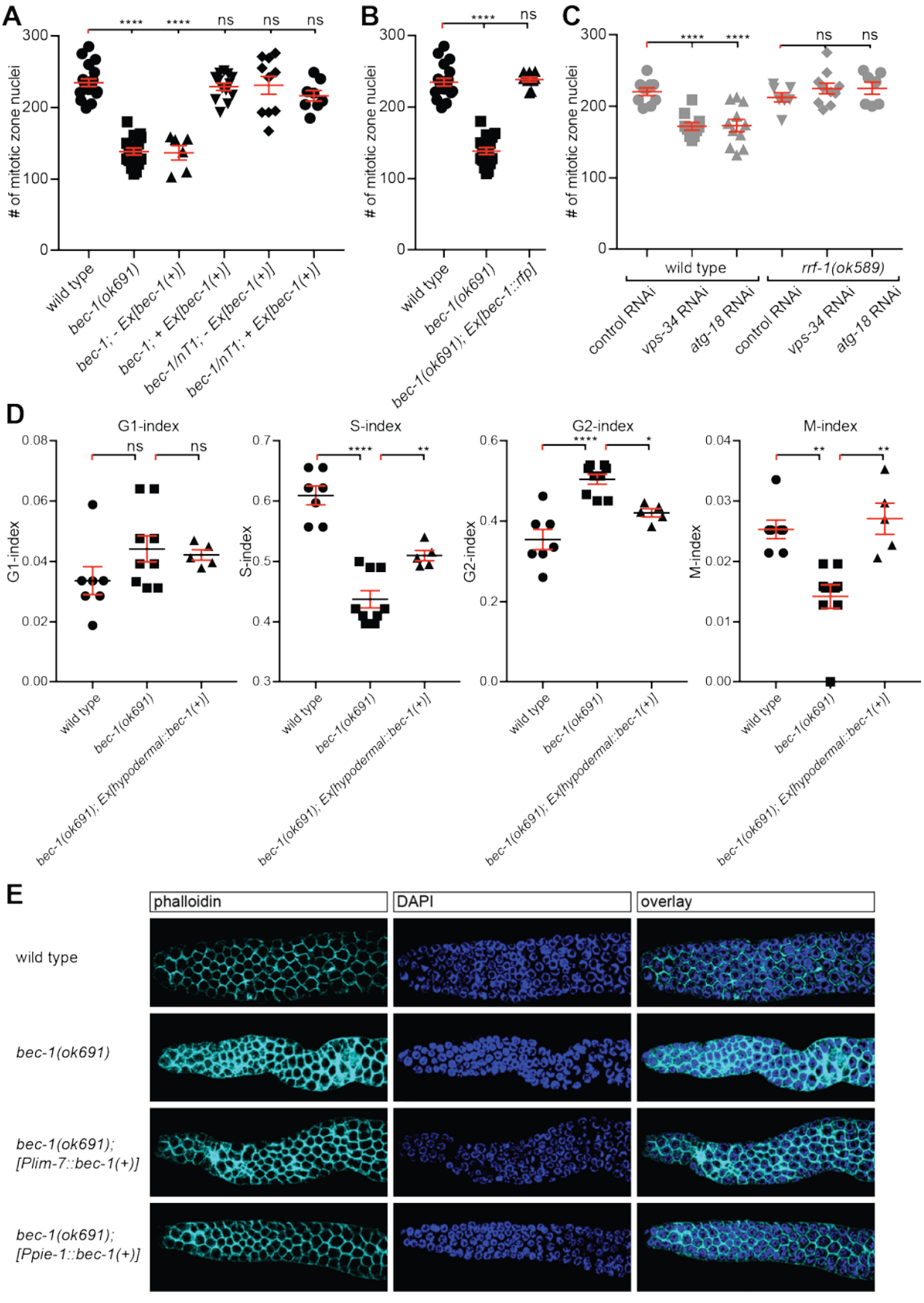
A
B
C
D
E
# of mitotic zone nuclei
wild type
bec-1(ok691)
bec-1; - Ex[bec-1(+)]
bec-1; + Ex[bec-1(+)]
bec-1/nT1; - Ex[bec-1(+)]
bec-1/nT1; + Ex[bec-1(+)]
bec-1(ok691); Ex[bec-1::rfp]
control RNAi
vps-34 RNAi
atg-18 RNAi
rrf-1(ok589)
G1-index
S-index
G2-index
M-index
bec-1(ok691); Ex[hypodermal::bec-1(+)]
phalloidin
DAPI
overlay
bec-1(ok691); [Plim-7::bec-1(+)]
bec-1(ok691); [Ppie-1::bec-1(+)]

Figure S4. Cellular focus of action for BEC-1/Beclin. ***Related to Figure 4.***
(A) Quantification of mitotic nuclei in the proliferative zone of wild-type, *bec-1(ok691)* homozygous, or *bec-1/nT1* heterozygous animals that carry (+) or do not carry (-) the extrachromosomal array expressing BEC-1 from its endogenous promoter, or **(B)** expressing the transgene izEx5, which consists of wild-type BEC-1 expressed from its endogenous promoter, fused with RFP.. The *bec-1(ok691)* homozygous animals segregated from the *bec-1/nT1* or *bec-1/nT1; Ex[bec-1(+), sur-5::gfp]* parents. **(C)** Quantification of the number of mitotic nuclei in wild-type or *rrf-1(ok589)* mutant animals RNAi depleted against *vps-34* or *atg-18*. Plasmid (L4440) served as a negative control. **(D)** Quantification of M-phase index**,** S-phase index, G1 index and G2 in wild-type and *bec-1(ok691)* mutants, and in *bec-1(ok691)* mutant that express the BEC-1 cDNA from a hypodermal (*dpy-7*) promoter (data for wild type and *bec-1(ok691)* is identical to the data in Figure 3D and shown for comparison only). **(E)** Representative confocal images of the extracted gonads stained with DAPI and Phalloidin stain to visualize the plasma membrane in wild type, *bec-1(ok691)* single mutant animals and *bec-1* animals expressing BEC-1 in the germ line under a *pie-1* promoter, and in sheath cells under a *lim-7* promoter. For (A), (B), (D), and (E), animals were grown at 15ºC, shifted to 20ºC as L3 larvae, and analyzed as young adults. For (C), animals grown at 15ºC, as L1 larvae shifted to 20ºC, and analyzed as young adults. For (A)-(E), results reflect the average of at least three biological replicates shown as the mean ±SEM (shown as error bars). Statistical significance was determined by one-way ANOVA with corrections for multiple comparisons using the method of Dunnett, and indicated as * P ≤0.05, ** P≤0.01, *** P≤0.001, **** P≤0.0001, ns - not significant.

Supplemental Experimental Procedures

Strains, plasmids and transgenes

Strains were generated for this study:
QU67: *bec-1(ok691)/nT1[qIs51]; izEx100[*P*dpy-7::bec-1(+), sur-5::GFP]*, QU68: *bec-1(ok691)/nT1[qIs51]; izEx101[*P*myo-3::bec-1(+), sur-5::GFP]*, QU71: *bec-1(ok691)/ nT1[qIs51]; izEx102[*P*rgef-1::bec-1(+), sur-5::GFP]*, QU134: *bec-1(ok691)/nT1[qIs51]; Ex[*P*glo-1::bec-1(+), rol-6(su1006)]*, QU155: *bec-1(ok691)/nT1[qIs51]; Ex[*P*glo-1::bec-1(+), rol-6(su1006)]*, QU135: *bec-1(ok691)/nT1[qIs51]; Ex[Prgef-1::bec-1(+), sur-5::GFP]*, QU137: *bec-1(ok691)/nT1[qIs51]; Ex[*P*dpy-7::bec-1(+), sur-5::GFP]*, QU136: *bec-1(ok691)/nT1[qIs51]; Ex[*P*myo-3::bec-1(+), sur-5::GFP]*, EB2589: *bec-1(ok691) IV/nT1 [qIs51] (IV,V); dzTi2[pie-1p::bec-1::mCherry::tbb-2 3'UTR +NeoR]V*, EB2590: *bec-1(ok691) IV/nT1 [qIs51] (IV,V); dzTi3[pie-1p::bec-1::mCherry::tbb-2 3'UTR +NeoR]V*, EB2591: *bec-1(ok691) IV/nT1 [qIs51] (IV,V); dzTi4[pie-1p::bec-1::mCherry::tbb-2 3'UTR +NeoR]V*, and EB2629: *bec-1(ok691) IV/nT1 [qIs51] (IV;V); Is[lim-7p::bec-1::mCherry::tbb-2 3'UTR + NeoR]*.

Other strains used in this study:
QU22: *bec-1(ok691); izEx5 [pAy39.1, bec-1::BEC-1::RFP]* [S1] [S2]**,** QU254: *bec-1(ok691); izEx6 [bec-1(+), pTG96 (sur-5::GFP)]* [S1], HZ1683: *him-5(e1490) V; atg-2(bp576) X* [S3], HZ1684: *atg-3(bp412) IV; him-5(e1490) V* [S4], HZ1687: *atg-9(bp564) him-5(e1490) V* [S3], HZ1691: *epg-8(bp251) I; him-5(e1490) V* [S5], DR466: *him-5(e1490)V*, MD701: *bcIs39[lim-7p::ced-1::GFP+lin-15]V, bec-1(ok691)/nT1*[*qIs51*]*; Ex[*P*ced-1::mCherry::bec-1(+), rol-6(su1006)]* [S6].

Plasmid construction

The pTB80 plasmid, (P*dpy-7*::gfp) [S7], containing the hypodermal *dpy-7* promoter and the *Hind*III and *Pst*I, was kindly provided by Oliver Hobert. The *bec-1* cDNA (verified by sequencing) was cloned into pTB80 using *Kpn*I and *Bsm*I (blunt end) to produce pAM200 [P*dpy-7*::BEC-1]. This pAM200 [P*dpy-7*::BEC-1] was injected at 10µg/ml together with pTG96 [*sur-5*::GFP] at 100µg/ml, into the *bec-1(ok691) IV/nT1 [qIs51]* (IV;V) strain, to generate *izEx100* [P*dpy-7*::BEC-1, pRF4], and the strain QU67: carrying *bec-1(ok691)/nT1*[qIs51]*; izEx100[*P*dpy-7::bec-1(+), sur-5::GFP]*.

The muscle expression plasmid pAM260 was designed to contain the *myo-3* promoter of pPD95_86.myo-3. To this construct, the *bec-1* cDNA fragment from pAM200 was cloned using *Kpn*I and *Bsm*I. The pAM260 [P*myo-3*::BEC-1] construct was injected at 10µg/ml, together with pTG96 [*sur-5*::GFP] at 100µg/ml, into *bec-1(ok691)*

IV/nT1 [qIs51] (IV;V) animals, to generate izEx101 [P*myo-3*::BEC-1, pTG96], and the strain QU68, carrying *bec-1(ok691)/nT1*[qIs51]*; izEx101[*P*myo-3::bec-1(+), sur-5::GFP]*.

The neuronal pAM240 [P*rgef-1*::BEC-1] construct consists of a fragment *Kpn*I to *Eag*I from plasmid pF25B3.3 cloned into pAM200, which contains the *bec-1* cDNA. pAM240 [P*rgef-1*::BEC-1] was injected into *bec-1(ok691) IV/nT1 [qIs51]* (IV;V) animals at 10µg/ml, together with pTG96 [sur-5::GFP] at 100µg/ml, to generate *izEx102* [P*rgef-1*::BEC-1, pTG96], and the strain QU71, which carries *bec-1(ok691)/ nT1*[qIs51]*; izEx102[*P*rgef-1::bec-1(+), sur-5::GFP]*.

For the intestinal expression of *bec-1*, the *bec-1* cDNA was amplified from pAM200 [P*dpy-7*::BEC-1], cloned into TOPO Kit and verified by sequencing. The *bec-1* cDNA containing *Age*I and *Eco*RV was cloned into pDS224 [P*glo-1*::mCherry] to form pAM400. pAM400 was injected into *bec-1(ok691) IV/nT1 [qIs51]* (IV;V) animals at 20µg/ml, together with the dominant roller marker pRF4 [*rol-6*(*su1006*)] at 100µg/ml, and *izEx103 [Pglo-1::BEC-1, pRF4]* was generated, and contained in strains QU134 and QU155: *bec-1(ok691)/nT1[qIs51]; Ex[*P*glo-1::bec-1(+), rol-6]*.

A *Pced-1::mCherry::bec-1* consists of a full-length *bec-1* cDNA as previously described [S6]. An extrachromosomal array was generated by injecting the plasmid containing the P*ced-1::mCherry::bec-1* into *bec-1*(*ok691*)/*nT1*[*qIs51*], with pRF4 [*rol-6*(*su1006*)]. This construct was previously shown to rescue the embryonic cell corpse engulfment phenotype in *bec-1* homozygous mutant animals [S6].

miniMos constructs

Two constructs were made to express *bec-1* in the germ line *[*P*pie-1p::bec-1::mCherry::tbb-2 3'UTR + NeoR]* and in the sheath cells *[*P*lim-7p::bec-1::mCherry::tbb-2 3'UTR + NeoR]*. In short, we used the strategy previously described by Frokjaer-Jensen et al. [S8]. A construct comprising the *bec-1* cDNA under the control of the *pie-1* or *lim-7* promoter, followed by the *tbb-2* 3' UTR, was assembled by Gibson assembly in the miniMos vector (*pCFJ910*- neoR),. The final plasmid P*pie-1p*::*bec-1::*mCherry::*tbb-2* (or P*lim-7p::bec-1::mCherry::tbb-2*) was injected (10 ng/µl) into the *bec-1(ok691) IV/nT1 [qIs51]* (IV;V) strain, with the following co-injection plasmids: *pGH8* (*Prab-3::mCherry::unc-54UTR*) at 20 ng/µl, pCFJ90 (*Pmyo-2:mCherry:unc-54UTR*) at 5 ng/µl, pCFJ104 (P*myo-3::mCherry::unc-54UTR*) at 20 ng/µl, pCFJ601 (P*eft-3::mos1 transposase::tbb-2UTR*) at 100 ng/µl, pMA122 (P*hsp16.41:peel-1:tbb-2UTR*) at 10 ng/µl. Three miniMos insertions of *bec-1(ok691) IV/nT1 [qIs51]* (IV;V); *Ti[*P*pie-1p::bec-1::mCherry::tbb-2 3'UTR + NeoR]* were identified and analyzed. One miniMos insertion of *bec-1(ok691) IV/nT1 [qIs51]* (IV;V); *Ti[*P*lim-7p::bec-1::mCherry::tbb-2 3'UTR + NeoR]* was identified and analyzed.

Microscopy

Fluorescent images were captured using a Leica TCS-SP5 laser-scanning confocal microscope. Z-stacks were taken at 1.5 µm steps. Images were collected by a PMT (photomultiplier tube) detector, processed in 3-D projection mode, and converted to TIFF format for analysis.

Staining and Immunofluorescence

Germ lines were analyzed by visualizing DAPI (Vectashield) stained gonads of whole worms [S9] and/or dissected gonads [S10]. For whole worm staining: animals were fixed in 95% ice-cold ethanol and stained with DAPI (Vectashield) mounting media. For extracted gonad analysis: gonads were extracted in phosphate-buffered saline solution (PBS) containing 0.25mM levamisole [S11], fixed in 2% PFA for 10min, blocked in PBS (1%BSA) for 30 min, and DAPI stained. For phalloidin staining PBS blocked gonads were stained with Phalloidin (ThermoFisher Scientific) 5µl in 200 µg PBS (1%BSA) for 20 min at room temperature, followed by 3 washes in PBS and DAPI stained. Animals or gonads were mounted on slides containing a 3% agarose pad for microscopy.

RNA interference

L4 animals were fed dsRNA expression bacteria and their progeny analyzed. Synchronization of F1 progeny, from RNAi treated animals, was achieved by a "wash-off" method, where parents are washed off the plates and the remaining eggs were allowed to hatch during a 2-hour period (modified protocol [S9]). Hatched L1 animals were transferred onto fresh RNAi plates (and grown at the specified temperature, and analyzed as young adults (with up

to 6 eggs per gonad), unless noted otherwise. HT115 *E. coli* that expressed target dsRNA were obtained from the Ahringer and Vidal libraries [S12, S13], and sequence verified.

5-ethynyl-2-deoxyuridine (EdU) labeling

NGM plates were seeded with small amounts of OP50 bacteria (50-100 µl) and grown overnight. The bacteria on plates were killed, by UV at 0.5J/sec for 10 min). 12 h later, an EdU solution (stock 300 µM) was applied to cover the entire lawn of the killed bacteria. After the EdU solution dried up, adult animals were placed on NGM plates and fed the dead bacteria covered with the EdU solution for 30 min, followed by the immediate dissection of gonads. Gonads were extracted in 0.25µM levamisole, fixed using 3.7% PFA for 10 min, permeabilized with 0.1% Triton X-100 in PBSB, blocked in PBSB for 30 min, and processed using the Click-IT EdU reaction (Molecular Probes), according to the manufacturer's protocol. Following the Click-IT reaction incubation, the gonads were antibody and DAPI stained, before imaging.

Measuring Mitotic, Synthesis, G1 and G2 phase Indexes

Gonads were extracted in PBS containing 0.25 mM levamisole [S11], fixed in 2% PFA for 10min, permeabilized with 0.1% Triton X-100 in PBSB, and blocked in PBSB (1%BSA) for 30 min. Extracted gonads were then stained with the anti-Phospho Histone H3 marker (Millipore) (1:500), for at least 4 hours at room temperature, followed by 3 X 15 min washes in PBSB and stained with a goat-anti-rabbit secondary antibody stain Alexa Fluor 488 or Alexa Fluor 564 (5µg/ml) (Life Technnologies), for at least 2 hours at room temperature, followed by 3 X 15 min washes in PBSB. As a final step, gonads were DAPI stained (using Vectashield) and mounted on slides with pads made of 3% agarose, for microscopy.

The mitotic index (M-phase index) was calculated as a ratio of phospho-Histone H3 positive cells in metaphase and anaphase (determined by nuclear anatomy), to the total number of nuclei in the proliferative zone [S14]. The Synthesis index (S-phase index) was calculated as a ratio of the EdU positive cells, to the total number of mitotic cells. The presence in the cell of any EdU staining (on individual chromosomes or all chromosomes) was scored as an EdU positive cell.

Mitotic cycling in the proliferative zone of *C. elegans* is continuous and lacks quiescent cells [S10], and it is assumed that all the progenitor cells in the mitotic zone are distributed between G1, S, G2 and M phases. To quantify G1 and G2 phases, images were processed in Image J and the pixel intensity of DAPI nuclear staining was calculated as the sum of all pixel intensities, within a manually drawn outline around each nucleus in the mitotic zone [S15]. G1 phase nuclei are classified by less DNA content than that of S-phase cells, and not in M-phase. G2 phase nuclei are classified by having DNA content greater than that of S-phase cells and not EdU positive.

Supplemental References

S1. Ruck, A., Attonito, J., Garces, K.T., Nunez, L., Palmisano, N.J., Rubel, Z., Bai, Z., Nguyen, K.C., Sun, L., Grant, B.D., et al. (2011). The Atg6/Vps30/Beclin 1 ortholog BEC-1 mediates endocytic retrograde transport in addition to autophagy in C. elegans. Autophagy *7*, 386-400.

S2. Rowland, A.M., Richmond, J.E., Olsen, J.G., Hall, D.H., and Bamber, B.A. (2006). Presynaptic terminals independently regulate synaptic clustering and autophagy of GABAA receptors in Caenorhabditis elegans. J Neurosci *26*, 1711-1720.

S3. Lu, Q., Yang, P., Huang, X., Hu, W., Guo, B., Wu, F., Lin, L., Kovacs, A.L., Yu, L., and Zhang, H. (2011). The WD40 repeat PtdIns(3)P-binding protein EPG-6 regulates progression of omegasomes to autophagosomes. Dev Cell *21*, 343-357.

S4. Tian, E., Wang, F., Han, J., and Zhang, H. (2009). epg-1 functions in autophagy-regulated processes and may encode a highly divergent Atg13 homolog in C. elegans. Autophagy *5*, 608-615.

S5. Yang, P., and Zhang, H. (2011). The coiled-coil domain protein EPG-8 plays an essential role in the autophagy pathway in C. elegans. Autophagy *7*, 159-165.

S6. Huang, S., Jia, K., Wang, Y., Zhou, Z., and Levine, B. (2013). Autophagy genes function in apoptotic cell corpse clearance during C. elegans embryonic development. Autophagy *9*, 138-149.

S7. Boulin, T., Pocock, R., and Hobert, O. (2006). A novel Eph receptor-interacting IgSF protein provides C. elegans motoneurons with midline guidepost function. Curr Biol *16*, 1871-1883.

S8. Frokjaer-Jensen, C., Davis, M.W., Sarov, M., Taylor, J., Flibotte, S., LaBella, M., Pozniakovsky, A., Moerman, D.G., and Jorgensen, E.M. (2014). Random and targeted transgene insertion in Caenorhabditis elegans using a modified Mos1 transposon. Nat Methods *11*, 529-534.

S9. Pepper, A.S., Killian, D.J., and Hubbard, E.J. (2003). Genetic analysis of Caenorhabditis elegans glp-1 mutants suggests receptor interaction or competition. Genetics *163*, 115-132.

S10. Crittenden, S.L., Leonhard, K.A., Byrd, D.T., and Kimble, J. (2006). Cellular analyses of the mitotic region in the Caenorhabditis elegans adult germ line. Mol Biol Cell *17*, 3051-3061.
S11. Francis, R., Barton, M.K., Kimble, J., and Schedl, T. (1995). gld-1, a tumor suppressor gene required for oocyte development in Caenorhabditis elegans. Genetics *139*, 579-606.
S12. Kamath, R.S., Fraser, A.G., Dong, Y., Poulin, G., Durbin, R., Gotta, M., Kanapin, A., Le Bot, N., Moreno, S., Sohrmann, M., et al. (2003). Systematic functional analysis of the Caenorhabditis elegans genome using RNAi. Nature *421*, 231-237.
S13. Rual, J.F., Hill, D.E., and Vidal, M. (2004). ORFeome projects: gateway between genomics and omics. Curr Opin Chem Biol *8*, 20-25.
S14. Maciejowski, J., Ugel, N., Mishra, B., Isopi, M., and Hubbard, E.J. (2006). Quantitative analysis of germline mitosis in adult C. elegans. Dev Biol *292*, 142-151.
S15. Seidel, H.S., and Kimble, J. (2015). Cell-cycle quiescence maintains Caenorhabditis elegans germline stem cells independent of GLP-1/Notch. Elife *4*.